Life Sciences 334 (2023) 122173

Contents lists available at ScienceDirect

Life Sciences

journal homepage: www.elsevier.com/locate/lifescie

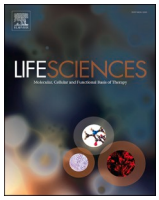

Applying HDACis to increase SSTR2 expression and radiolabeled DOTA-TATE uptake: from cells to mice

Maria J. Klomp [a,b], Lilian van den Brink [a], Peter M. van Koetsveld [b], Corrina M.A. de Ridder [a,c], Debra C. Stuurman [a,c], Clemens W.G.M. Löwik [a], Leo J. Hofland [b], Simone U. Dalm [a,*]

[a] Department of Radiology and Nuclear Medicine, Erasmus MC, 3015 GD Rotterdam, The Netherlands
[b] Department of Internal Medicine, Division of Endocrinology, Erasmus MC, 3015 GD Rotterdam, The Netherlands
[c] Department of Experimental Urology, Erasmus MC, 3015 GD Rotterdam, The Netherlands

ARTICLE INFO

Keywords:
Epigenetic drugs
Histone deacetylase inhibitors
Octreotate
Neuroendocrine tumors

ABSTRACT

Aims: The aim of our study was to determine the effect of histone deacetylase (HDAC) inhibitors (HDACis) on somatostatin type-2 receptor (SSTR2) expression and [^{111}In]In-/[^{177}Lu]Lu-DOTA-TATE uptake *in vitro* and *in vivo*.

Materials and methods: The human cell lines NCI-H69 (small-cell lung carcinoma) and BON-1 (pancreatic neuroendocrine tumor) were treated with HDACis (*i.e.* entinostat, mocetinostat (MOC), LMK-235, CI-994 or panobinostat (PAN)), and *SSTR2* mRNA expression levels and [^{111}In]In-DOTA-TATE uptake were measured. Furthermore, vehicle- and HDACi-treated NCI-H69 and BON-1 tumor-bearing mice were injected with radiolabeled DOTA-TATE followed by biodistribution studies. Additionally, *SSTR2* and *HDAC* mRNA expression of xenografts, and of NCI-H69, BON-1, NCI-H727 (human pulmonary carcinoid) and GOT1 (human midgut neuroendocrine tumor) cells were determined.

Key findings: HDACi treatment resulted in the desired effects *in vitro*. However, no significant increase in tumoral DOTA-TATE uptake was observed after HDACi treatment in NCI-H69 tumor-bearing animals, whereas tumoral *SSTR2* mRNA and/or protein expression levels were significantly upregulated after treatment with MOC, CI-994 and PAN, *i.e.* a maximum of 2.1- and 1.3-fold, respectively. Analysis of PAN-treated BON-1 xenografts solely demonstrated increased *SSTR2* mRNA expression levels. Comparison of *HDACs* and *SSTR2* expression in BON-1 and NCI-H69 xenografts showed a significantly higher expression of 6/11 HDACs in BON-1 xenografts. Of these HDACs, a significant inverse correlation was found between *HDAC3* and *SSTR2* expression (Pearson $r = -0.92$) in the studied cell lines.

Significance: To conclude, tumoral uptake levels of radiolabeled DOTA-TATE were not enhanced after HDACi treatment *in vivo*, but, depending on the applied inhibitor, increased SSTR2 expression levels were observed.

1. Introduction

The somatostatin type-2 receptor (SSTR2) is abundantly expressed in the endocrine system and is physiologically involved in inhibiting hormone secretion, cell proliferation and migration, as well as angiogenesis [1]. Due to the frequent overexpression of SSTR2 on neuroendocrine tumor (NET) cells, it forms a pivotal target for therapy using somatostatin analogues (SSAs) or radiolabeled SSAs, *i.e.* [[^{177}Lu]Lu-DOTA^{0},Tyr^{3}]octreotate ([^{177}Lu]Lu-DOTA-TATE) [2]. Treatment with (radiolabeled) SSAs reduces symptoms associated with hormonal hypersecretion [3,4] and inhibits tumor growth, thereby improving clinical outcomes for NET patients [5–8]. However, a substantial number of patients do not benefit from this therapy, demonstrating the need for improvement for which multiple approaches are currently under

Abbreviations: %ID/g, percentage injected dose per gram tissue; [^{177}Lu]Lu-DOTA-TATE, [[^{177}Lu]Lu-DOTA^{0},Tyr^{3}]octreotate; ^{111}In, indium-111; ^{177}Lu, lutetium-177; DAB, 3,3′-diaminobenzidine; ENT, entinostat; FBS, fetal bovine serum; HBSS, Hanks' balanced salt solution; HDAC, histone deacetylase; HDACis, histone deacetylase inhibitors; MOC, mocetinostat; NET, neuroendocrine tumor; PAN, panobinostat; PAS^{+}, periodic acid-Schiff diastase; PBS, phosphate buffered saline; SD, standard deviation; SSA, somatostatin analogue; SSTR2, somatostatin type-2 receptor.

* Corresponding author at: Department of Radiology & Nuclear Medicine, Room NA2503, Dr. Molewaterplein 50, 3015GD, Rotterdam, The Netherlands.
E-mail address: s.dalm@erasmusmc.nl (S.U. Dalm).

https://doi.org/10.1016/j.lfs.2023.122173
Received 16 August 2023; Received in revised form 1 October 2023; Accepted 10 October 2023
Available online 29 October 2023

investigation [9].

One of the approaches is upregulation of the target receptor SSTR2 using epigenetic drugs. There is growing evidence for the involvement of the epigenetic machinery in both NET pathogenesis and in regulating SSTR2 expression [10–13]. As a result, epigenetic drugs are extensively being investigated as a method to increase SSTR2 expression. Promising results were obtained when applying the histone deacetylase inhibitor (HDACi) valproic acid *in vitro* [14–16]. However, our previous study with mice bearing a tumor derived from the well-known SSTR2 expressing NCI-H69 cell line showed that valproic acid led to increased uptake of [^{177}Lu]Lu-DOTA-TATE but did not increase tumoral SSTR2 expression levels [17]. Instead, the observed increase in radiolabeled SSA uptake was caused by an enhanced radiotracer blood circulation time, which was associated with kidney damage observed after HDACi treatment. Related hereto, Refardt et al. reported on the combination of valproic acid with the DNA methyltransferase inhibitor hydralazine, which did also not result in an increased tumoral uptake of radiolabeled DOTA-TATE in advanced NET patients with low baseline SSTR2 expression [18]. However, in contrast, in a small study with metastatic midgut NET patients, it was demonstrated that treatment with the HDACi vorinostat did result in an increased uptake of [^{68}Ga]Ga-DOTATOC [19]. Besides vorinostat tested in patients, there are other HDACis which demonstrated convincing results on SSTR2 upregulation *in vitro* [20–23]. Together, this gives the impression that HDACi-induced SSTR2 upregulation and enhanced uptake of radiolabeled SSA might be effectively achieved under the appropriate conditions, potentially resulting in an improved therapeutic response to [^{177}Lu]Lu-DOTA-TATE therapy.

Various preclinical studies demonstrated SSTR2 upregulation after treatment with other HDACis *in vitro*, but *in vivo* studies demonstrating successful HDACi-induced SSTR2 upregulation are lacking. Therefore, our aim was to screen a panel of HDACis *in vivo* using mice with a tumor derived from the previously mentioned NCI-H69 cells and the human pancreatic NET cell line BON-1, in order to select potent epigenetic drugs for increased radiolabeled DOTA-TATE uptake *via* SSTR2 upregulation. The potency of these HDACis might differ because these inhibitors target different, and some even multiple, classes of HDAC enzymes [24,25]. Additionally, we aimed to gain more insight into the association between HDAC and SSTR2 expression by measuring mRNA expression levels in different models, *i.e.* cell lines and xenografts.

2. Materials and methods

2.1. Cell culture

The human small-cell lung carcinoma cell line NCI-H69 (European Collection of Authenticated Cell Cultures) was cultured in RPMI-medium 1640 + GlutaMAX-I (Gibco, Breda, The Netherlands), supplemented with 10 % (*v/v*) fetal bovine serum (FBS, Gibco), 100 U/mL penicillin and 100 μg/mL streptomycin (Sigma-Aldrich). The human pancreatic NET cell line BON-1 (kind gift of Dr. Townsend, University of Texas Medical branch, Galveston, TX, USA) was cultured in DMEM/F-12 (1:1) (Gibco), supplemented with 10 % (*v/v*) FBS (Sigma-Aldrich), 2 mM L-glutamine (Gibco), 1.25 mg/L fungizone (Bristol Myers Squibb) and 100 U/mL penicillin (Sigma-Aldrich). Both cell lines were passaged once a week up to 20 passages and maintained in a humidified atmosphere (37 °C, 5 % CO_2). The human pulmonary carcinoid cell line NCI-H727 (ATCC CRL-5815) and human midgut NET cell line GOT1 (kind gift of Ola Nilsson, Sahlgrenska Cancer Center, University of Gothenburg, Sweden) were cultured as previously described [23]. A common characteristic of these four cell lines is the expression of SSTR2; BON-1 cells express low levels, NCI-H727 intermediate levels, and NCI-H69 and GOT1 express high levels of SSTR2.

2.2. Dose-response studies

IC_{50} values of all HDACis were determined following 72 h of treatment. For this, NCI-H69 or BON-1 cells were plated in 96-well plates, and HDACis entinostat (ENT, Sigma-Aldrich), mocetinostat (MOC, Bio-Connect B.V.), LMK-235 (AbMole Bioscience Inc.), CI-994 (Sigma) or panobinostat (PAN, Bio-Connect B.V.) were added 24 h after plating. All HDACis were dissolved in 40 % DMSO, which served as the vehicle (final concentration was 0.4 % DMSO). All HDACis were tested in NCI-H69 cells, and PAN was the only tested HDACi in BON-1 cells. After 72 h of HDACi treatment, we measured the cell viability by performing a CellTiter-Glo® 3D assay (Promega) according to manufacturer instructions. A SpectraMax iD3 plate reader (Molecular Devices) was used to measure the luminescent signal, and the cell viability was normalized to vehicle-treated cells. The resulting IC_{50} dose was used to treat NCI-H69 and BON-1 cells prior to [^{111}In]In-DOTA-TATE uptake studies and *SSTR2* mRNA analysis. A detailed protocol on HDACi treatment can be found in the Supplemental Appendix.

2.3. DOTA-TATE radiolabeling

DOTA-TATE was radiolabeled with indium-111 (^{111}In) or lutetium-177 (^{177}Lu) following the previously described method [17,26]. For *in vitro* uptake studies, [^{111}In]In-DOTA-TATE (40 MBq/1 nmol) was used. For *in vivo* studies with NCI-H69 tumor-bearing animals, [^{177}Lu]Lu-DOTA-TATE (100 MBq/1 nmol) was used and for studies with BON-1 tumor-bearing animals, we used [^{111}In]In-DOTA-TATE (100 MBq/1 nmol) to ensure the emission of sufficient gamma photons enabling accurate gamma counter measurements in this model as BON-1 cells are characterized by low SSTR2 expression levels and a relatively low uptake of radiolabeled DOTA-TATE was thus expected.

2.4. [^{111}In]In-DOTA-TATE uptake studies

Uptake studies were performed with vehicle- or HDACi-treated NCI-H69 and BON-1 cells to determine whether the uptake of radiolabeled DOTA-TATE was increased after epigenetic drug treatment. After 72 h of HDACi treatment at the IC_{50} dose, the [^{111}In]In-DOTA-TATE uptake was determined which was expressed as the percentage specific uptake of the added dose per milligram DNA (specific uptake/mg DNA). To investigate whether the observed effects were time-dependent, uptake studies were also performed 4 and 24 h after start of HDACi treatment at the IC_{50} dose that was determined after 72 h treatment. A detailed protocol can be found in the Supplemental Appendix.

2.5. Animal model

All animal experiments were approved by the animal welfare committee of the Erasmus MC and were conducted in agreement with the institutional guidelines. Male NMRI-Foxn1 nu/nu mice (5–8 weeks, Janvier) were housed in individually ventilated cages with *ad libitum* access to water and food. Before the start of the experiment, animals were left to acclimatize for 1 week. Mice were subcutaneously injected on the right shoulder with NCI-H69 cells (10×10^6 cells in 100 μL Hanks' Balanced Salt Solution (HBSS, Gibco)) or BON-1 cells (7.5×10^6 cells in 100 μL HBSS). After inoculation, tumor size was measured twice a week and tumor volume was calculated according to the following formula: π/6 (tumor length * tumor width) ^ (3/2). At the start of the experiment, the average tumor volumes were 198.1 ± 60.6 mm^3 and 199.6 ± 80.1 mm^3 for NCI-H69 and BON-1 xenografts, respectively. Information on experimental groups, *i.e.* tumor volume, body weight and the number of animals per group, are described in Tables S1 and S2.

2.6. Biodistribution studies

To determine the effect of HDACi treatment on radiolabeled DOTA-

TATE uptake, biodistribution studies were performed. Animals were injected daily with HDACis or the respective vehicle on three consecutive days. Details such as vehicle, route of administration and dose are described in Table 1. The selected HDACi doses and routes of administration were chosen based on previously published studies reporting HDACi-induced changes in the epigenetic profile [27–31]. All HDACis were tested in NCI-H69 tumor-bearing animals, whereas only PAN was tested in BON-1 tumor-bearing animals. Two hours after the last HDACi or vehicle injection, NCI-H69 and BON-1 tumor-bearing mice were intravenously injected with, respectively, 5 MBq/200 pmol/200 μL [^{177}Lu]Lu-DOTA-TATE (5.20 ± 0.17 MBq) or 20 MBq/200 pmol/200 μL [^{111}In]In-DOTA-TATE (19.89 ± 0.70 MBq), with or without an excess of unlabeled DOTA-TATE (10 nmol). Four hours after radiotracer injection, blood and organs were collected to determine the percentage injected dose per gram of tissue (%ID/g). More details can be found in the Supplemental Appendix. Of note, three NCI-H69 xenografted animals were excluded from the biodistribution study and the subsequent follow-up analyses due to technical issues. This concerned one animal of the MOC non-blocked group, the ENT non-blocked group and the respective vehicle non-blocked group.

2.7. SSTR2 and HDAC mRNA expression levels

RNA isolation, cDNA synthesis and RT-qPCR were performed as previously described [23], to measure *SSTR2* mRNA expression relative to three references genes (GUSB, HPRT1, ACTB). In addition to *SSTR2* mRNA expression levels, the mRNA expression levels of *HDAC1* to *HDAC11* were measured following the same method and using the primers described in Table S3.

2.8. SSTR2 protein expression levels

Formalin-fixed tumors of NCI-H69 and BON-1 tumor-bearing animals treated with HDACi or the respective vehicle were paraffin-embedded and subsequently an SSTR2 immunohistochemistry was performed as previously described [17]. The 3,3′-diaminobenzidine (DAB) intensity per area was quantified using the Cell Profiler software (Version 4.0.7) [32].

Table 1
Experimental details of HDACi treatment, including details on the solvent (vehicle), the route of administration and the applied dose expressed as milligram per kilogram of body weight (mg/kg body weight). All HDACis and solvents were purchased from Bio-Connect B.V. (Huissen, The Netherlands).

HDACi	Solvent/vehicle	Route of administration	Dose (mg/kg body weight)
ENT	2 % (*v*/*v*) DMSO 30 % (*v*/*v*) PEG300 68 % (*v*/*v*) H_2O	Oral gavage	20
MOC	2 % (*v*/*v*) DMSO 30 % (*v*/*v*) PEG300 68 % (*v*/*v*) H_2O	Oral gavage	90
LMK-235	5 % (*v*/*v*) DMSO 30 % (*v*/*v*) PEG300 5 % (*v*/*v*) Tween-80 60 % (*v*/*v*) H_2O	Intraperitoneal injection	20
CI-994	5 % (*v*/*v*) DMSO 40 % (*v*/*v*) PEG-300 55 % (*v*/*v*) H_2O	Intraperitoneal injection	35
PAN	2 % (*v*/*v*) DMSO 48 % (*v*/*v*) PEG-300 2 % (*v*/*v*) Tween-80 48 % (*v*/*v*) H_2O	Intraperitoneal injection	10

2.9. Renal tubular damage

Formalin-fixed kidneys of NCI-H69 and BON-1 tumor-bearing animals treated with PAN or its respective vehicle were paraffin-embedded, followed by a periodic acid-Schiff diastase (PAS^+) staining on the resulting sections. Subsequently, the sections were blindly scored for tubular damage using a 5-point scale, according to previously described methods [17].

2.10. Statistics

Statistical analysis was performed using GraphPad Prism version 9. Differences were considered statistically significant at $p < 0.05$, unless stated otherwise. All results are represented as mean ± standard deviation (SD). The *in vitro* data are representative for two independent biological experiments measuring three technical replicates per experiment, and the number of animals used for the *in vivo* studies can be found in Tables S1 and S2. To determine the IC_{50} value, a Fit Spline/LOWESS curve was plotted. A Shapiro-Wilk test was used to test the normality of the data. Depending on the normality of the data, a parametric or non-parametric test was performed, using an unpaired *t*-test or a One-Way ANOVA using the Dunnett's or a Tukey's multiple comparisons test as follow-up test, performing one test per time point, per organ or per primer. For the association between *SSTR2* and *HDAC* expression, a Spearman or Pearson correlation analysis was performed depending on the normality of the data. The *p*-values of the correlation analysis were corrected using a Bonferroni correction.

3. Results

3.1. In vitro effects of HDACi treatment in NCI-H69 cells

After treating NCI-H69 cells for 72 h with the HDACis, the cell viability was measured providing an IC_{50} value of 3.1×10^{-7} M, 4.2×10^{-7} M, 1.2×10^{-8} M, 4.8×10^{-7} M and 4.0×10^{-6} M for ENT, MOC, PAN, LMK-235 and CI-994, respectively (Fig. S1). Four hours after start of treatment at the IC_{50} dose, the uptake of [^{111}In]In-DOTA-TATE was significantly increased for PAN and LMK-235; a 1.3-fold increased uptake was measured for both HDACis ($p = 0.0003$ and $p = 0.0002$, respectively). Twenty-four hours after treatment, in addition to PAN and LMK-235 for which the uptake increased even further, treatment with all other HDACis also led to significant increased radiolabeled SSA uptake. At 24 h, the increase in uptake ranged between 1.4-fold and 2.2-fold with MOC and LMK-235 having the lowest and highest increase, respectively (Fig. 1a). Similarly, *SSTR2* mRNA expression levels measured 24 h after start of HDACi treatment were also all significantly increased, reaching a maximum increase of 2.1-fold ($p < 0.0001$) after LMK-235 treatment (Fig. 1b). Surprisingly, 72 h after constant exposure to the HDACis, the uptake of radiolabeled DOTA-TATE was no longer significantly enhanced (Fig. 1a).

3.2. Effects of HDACi in NCI-H69 tumor-bearing animals

Since *in vitro* results demonstrated that SSTR2 expression was quickly induced after HDACi exposure, animals were treated for a relatively short period, *i.e.* daily on three consecutive days. Despite these well-considered choices, *ex vivo* biodistribution data of NCI-H69 tumor-bearing animals showed that HDACi treatment did not result in a significant increased tumoral uptake of [^{177}Lu]Lu-DOTA-TATE in comparison to vehicle-treated animals (Fig. S2, Tables S4–S7). Although a trend towards an increased uptake was observed for the majority of HDACis (all except for LMK-235), results did not reach statistical significance. However, after MOC, PAN and CI-994 treatment, a significantly increased tumoral *SSTR2* mRNA expression level was measured, *i.e.* an increase of 1.5- ($p = 0.005$), 1.6- ($p = 0.0005$) and 2.1-fold ($p < 0.0001$), respectively (Fig. 2a–d). Additionally, SSTR2 protein

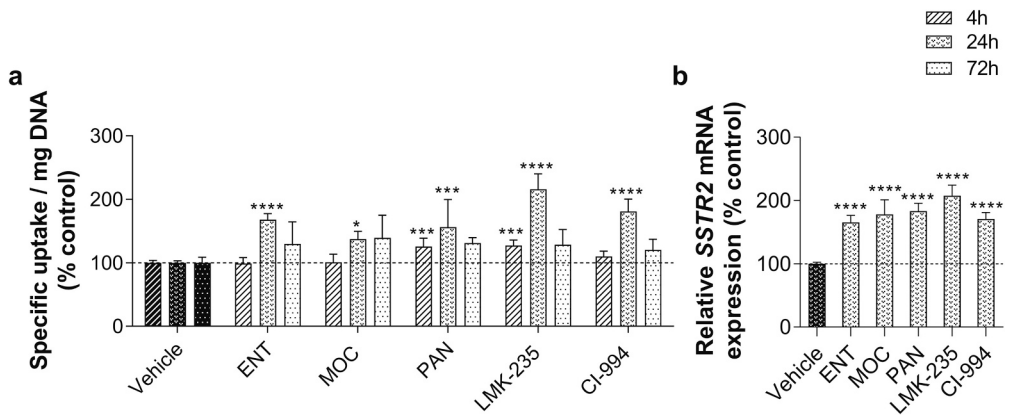

Fig. 1. (a) [^{111}In]In-DOTA-TATE uptake in vehicle- and HDACi-treated NCI-H69 cells measured 4, 24 and 72 h after start of HDACi treatment. Data is expressed as specific uptake/milligram DNA (specific uptake/mg DNA). (b) *SSTR2* mRNA expression levels in vehicle- and HDACi-treated NCI-H69 cells, measured 24 h after start of HDACi treatment. All results were normalized to vehicle-treated cells. $*p < 0.05$, $***p < 0.001$, $****p < 0.0001$.

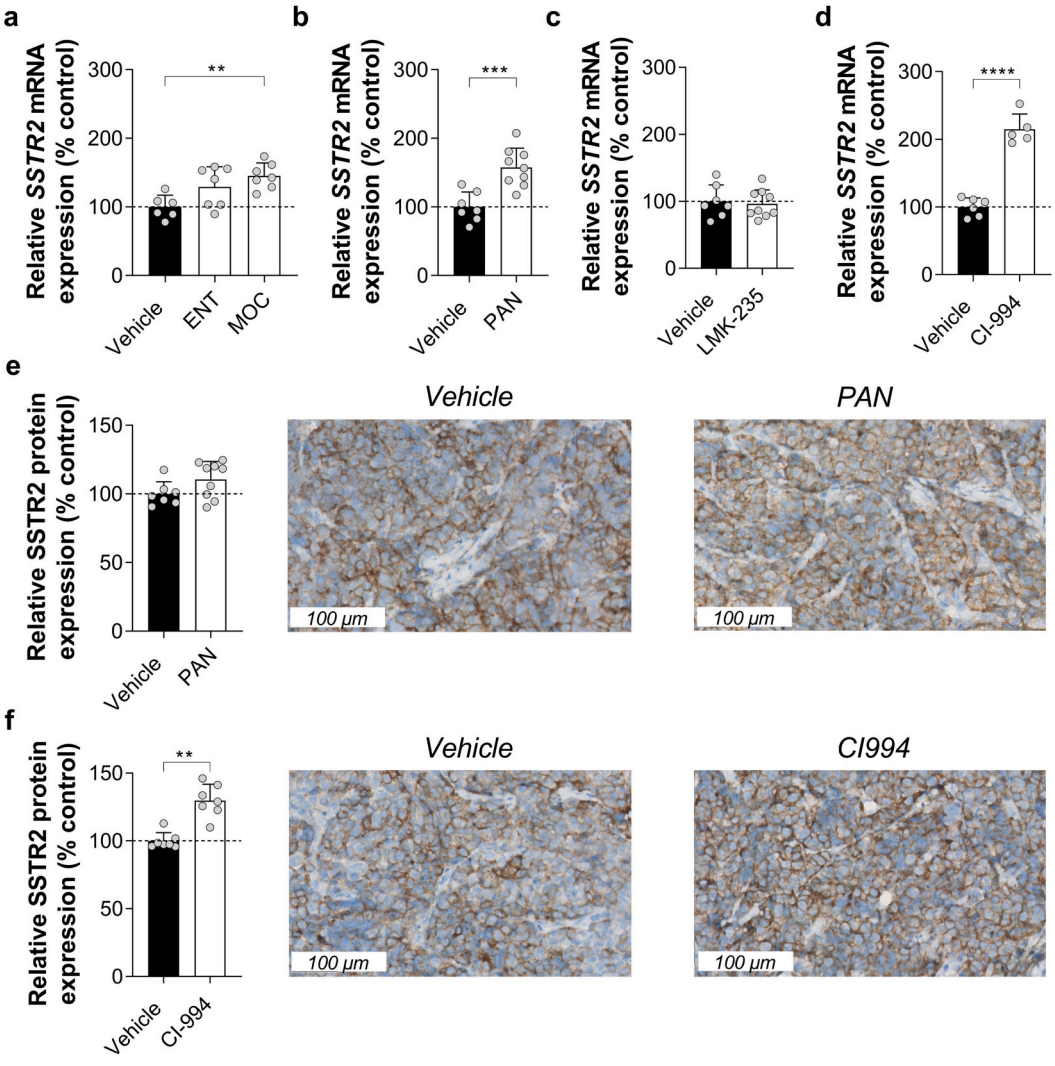

Fig. 2. *SSTR2* mRNA expression levels in vehicle- and HDACi-treated NCI-H69 xenografts; (a) entinostat (ENT) and mocetinostat (MOC), (b) panobinostat (PAN), (c) LMK-235 and (d) CI-994. Quantification of SSTR2 protein expression level and representative images of SSTR2 immunohistochemistry in vehicle- and HDACi-treated NCI-H69 xenografts; (e) PAN and (f) CI-994. All results were normalized to vehicle-treated animals. $**p < 0.01$, $***p < 0.001$, $****p < 0.0001$.

expression levels were quantified in tumors of PAN- and CI-994-treated animals, and compared to the levels measured in the respective vehicles. The SSTR2 staining intensity per area was non-significantly increased with a factor of 1.1 ($p = 0.0897$) after PAN treatment (Fig. 2e), and significantly increased by 1.3-fold ($p = 0.0012$) after CI-994 treatment (Fig. 2f).

Of note, results of the specificity study showed that the uptake of [^{177}Lu]Lu-DOTA-TATE could be blocked by co-injection of an excess of unlabeled DOTA-TATE demonstrating receptor specificity of radiolabeled SSA uptake in all experimental groups (Fig. S2, Tables S4–S7).

3.3. In vitro effects of PAN treatment in BON-1 cells

In order to exclude possible model-dependent outcomes, the effect of PAN in animals xenografted with the lower SSTR2-expressing BON-1 cell line was also evaluated. First, the effect of the HDACi was examined *in vitro*, demonstrating an IC_{50} value of 5.7×10^{-8} M (Fig. 3a). Treatment at this IC_{50} increased the radiolabeled SSA uptake significantly already 4 h after start of treatment, *i.e.* 1.6-fold ($p = 0.004$) (Fig. 3b). This increased even further to 5.1- ($p = 0.0002$) and 4.2-fold ($p < 0.0001$) after 24 and 72 h of treatment, respectively. No statistically significant difference was found between the two late time points ($p = 0.276$). Therefore *SSTR2* mRNA expression levels were only measured after 24 h of treatment, showing a 5.5-fold increased *SSTR2* mRNA expression level compared to vehicle-treated cells (Fig. 3c).

3.4. Effects of PAN in BON-1 tumor-bearing animals

Using the same treatment regimen as for NCI-H69 xenografts, BON-1 tumor-bearing animals were treated with PAN or its respective vehicle. *Ex vivo* biodistribution studies showed a tumoral uptake of 1.26 ± 0.35 %ID/g for vehicle-treated and 1.49 ± 0.30 %ID/g for PAN-treated BON-1 tumor-bearing animals ($p = 0.520$, Fig. 4a, Table S8). Thus, similar to the observations in the biodistribution study using NCI-H69 tumor-bearing animals, no significant increase in radiolabeled SSA uptake after HDACi treatment was observed in this model. *SSTR2* mRNA expression levels were significantly increased 2.0-fold ($p = 0.003$) after PAN treatment (Fig. 4b), and quantification of tumoral SSTR2 protein expression levels demonstrated no increase in SSTR2 staining intensity per area after epigenetic drug treatment ($p = 0.568$) (Fig. 4c).

Of note, we observed a slight increase in both the radioactivity measured in the blood ($p = 0.076$) and in uptake of several background organs after PAN treatment, including the kidneys in which the radioactivity uptake increased from 4.26 ± 0.67 %ID/g in vehicle-treated animals to 6.32 ± 1.29 %ID/g in PAN-treated animals ($p = 0.045$). A similar kidney uptake pattern was observed for the animals receiving an excess of unlabeled DOTA-TATE, *i.e.* 4.08 ± 0.66 %ID/g and 7.21 ± 2.31 %ID/g, respectively ($p = 0.037$). In addition to this, we observed that, in comparison to NCI-H69 tumor-bearing animals, the physiological uptake of radiolabeled DOTA-TATE was lower for BON-1 tumor-bearing animals in several background organs (*e.g.* GI tract ($p < 0.0001$) and pancreas ($p < 0.001$), Tables S5 and S8). Moreover, the radioactivity uptake in the kidneys was higher, *i.e.* 3.02 ± 1.00 and 4.26 ± 0.67 %ID/g in vehicle-treated NCI-H69 and BON-1 tumor-bearing animals ($p < 0.05$), respectively.

3.5. Kidney tubular damage of PAN-treated NCI-H69 and BON-1 tumor-bearing animals

Due to the increase in radiotracer uptake in the kidneys observed in PAN-treated BON-1 tumor-bearing animals in comparison to vehicle-treated animals, kidneys of all mice (*i.e.* NCI-H69 and BON-1 tumor-bearing animals) treated with PAN or the respective vehicle were analyzed for renal tubular damage. For both models, there was no significant increase in the average damage score in response to PAN treatment, *i.e.* 1.0 ± 0.8 *versus* 1.4 ± 0.5 for vehicle- and PAN-treated NCI-H69 tumor-bearing animals, and 0.1 ± 0.3 *versus* 0.1 ± 0.3 for vehicle- and PAN-treated BON-1 tumor-bearing animals, respectively (Table S9).

3.6. The association between SSTR2 and HDAC expression levels

To better interpret the findings described above, we measured *SSTR2* and *HDAC* mRNA expression of NCI-H69 and BON-1 xenografts. BON-1 xenografts had significantly lower *SSTR2* expression levels in comparison to NCI-H69 xenografts. Moreover, the HDACs were also differentially expressed in the two xenografts (Fig. 5); a significantly higher expression of *HDAC1*, *HDAC3*, *HDAC4*, *HDAC7*, *HDAC10* and *HDAC11* was measured in BON-1 xenografts in comparison to the expression in NCI-H69 xenografts. In contrast, the expression of *HDAC5* and *HDAC9* was significantly lower in BON-1 xenografts.

To investigate the association between SSTR2 expression and HDAC profiles, mRNA expression levels were measured in four cell lines (*i.e.* BON-1, NCI-H727, GOT1 and NCI-H69). First, we compared the HDAC expression pattern of BON-1 and NCI-H69 cells and xenografts to investigate whether the HDAC pattern was maintained from cell lines to xenografts, demonstrating that this was mostly the case (Fig. 5, S3). Therefore, *HDAC* and *SSTR2* mRNA expression levels measured in the four cell lines were correlated, thereby focusing on the six HDACs that were significantly higher expressed in BON-1 xenografts than in NCI-H69 xenografts (Fig. S4). It was demonstrated that HDAC7 and HDAC10 showed a trend towards a positive correlation with *SSTR2* mRNA expression levels, whereas HDAC1, HDAC3 and HDAC11 demonstrated inverse associations. Statistical significance was only reached between *HDAC3* and *SSTR2* expression levels (Pearson $r = -0.92$, $p = 0.0002$).

4. Discussion

Despite convincing preclinical *in vitro* results, *in vivo* studies showing the success of various HDACis in upregulating SSTR2, including enhanced uptake of [^{177}Lu]Lu-DOTA-TATE, are still lacking. For this

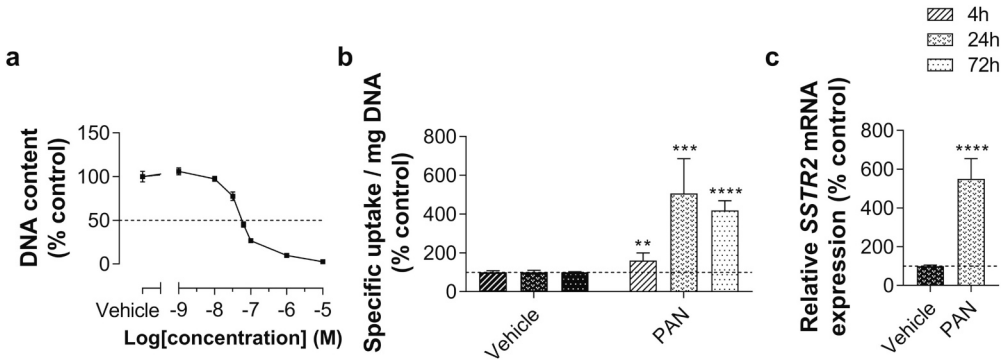

Fig. 3. (a) Dose-response curve of panobinostat (PAN) in BON-1 cells. (b) [^{111}In]In-DOTA-TATE uptake in vehicle- and PAN-treated BON-1 cells measured 4, 24 and 72 h after start of treatment. Data is expressed as specific uptake/milligram DNA (specific uptake/mg DNA) (c) *SSTR2* mRNA expression levels in vehicle- and PAN-treated BON-1 cells analyzed 24 h after start of treatment. All results were normalized to vehicle-treated cells. $^{**}p < 0.01$, $^{***}p < 0.001$, $^{****}p < 0.0001$.

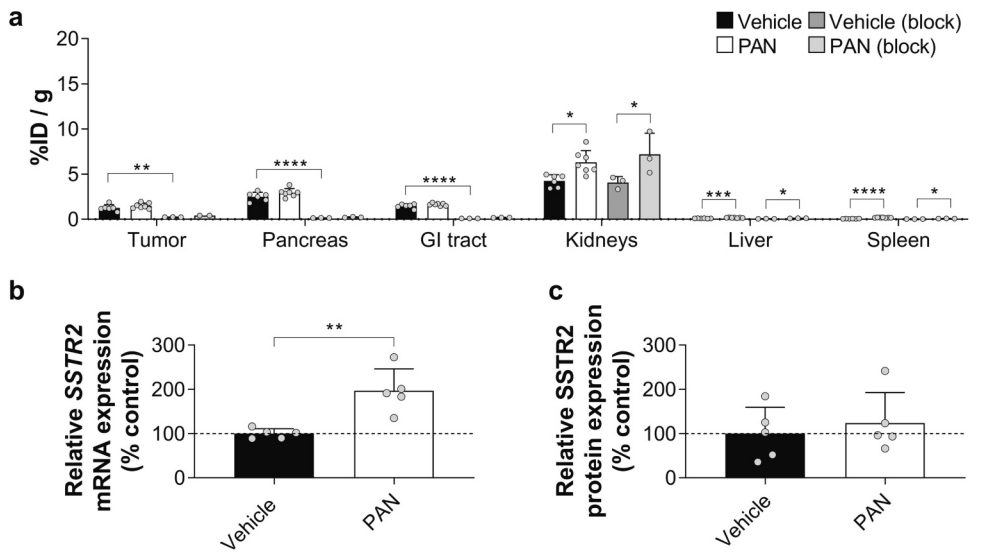

Fig. 4. (a) [^{111}In]In-DOTA-TATE uptake expressed as percentage injected dose per gram of tissue (%ID/g) in vehicle- and panobinostat (PAN) treated BON-1 xenografts. Block groups received an excess of unlabeled DOTA-TATE. (b) *SSTR2* mRNA and (c) SSTR2 protein expression levels in vehicle- and PAN-treated BON-1 xenografts. All results were normalized to vehicle-treated animals. *$p < 0.05$, **$p < 0.01$, ***$p < 0.001$, ****$p < 0.0001$.

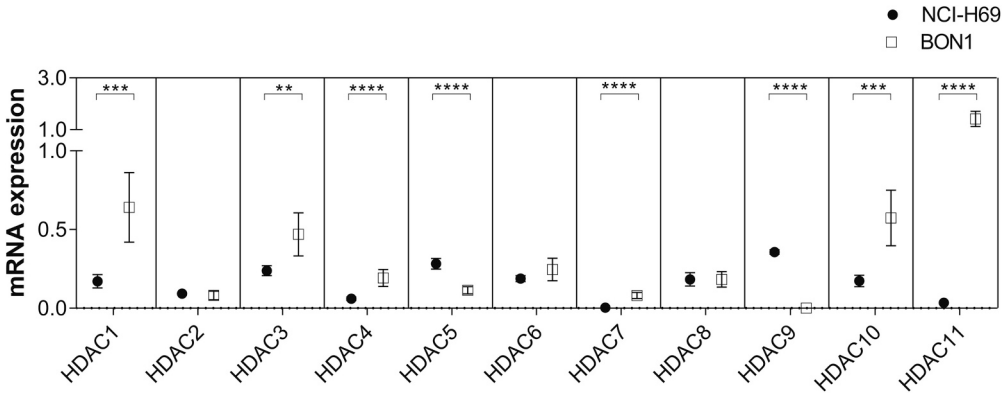

Fig. 5. *HDAC* mRNA expression levels in NCI-H69 and BON-1 xenografts. mRNA levels are expressed relative to three reference genes. **$p < 0.01$, ***$p < 0.001$, ****$p < 0.0001$.

reason, we screened multiple HDACis in NCI-H69 and BON-1 tumor-bearing animals.

First, we confirmed the *in vitro* effects of HDACi treatment in NCI-H69 cells. Uptake studies demonstrated a time-dependent effect, with the strongest effects observed 24 h after start of HDACi treatment. After 72 h of HDACi treatment, however, effects were reduced, which is possibly a consequence of degradation of the HDACis. In line with the significantly increased uptake observed after 24 h of treatment, *SSTR2* mRNA expression levels were increased as well. Both the uptake of radiolabeled DOTA-TATE and *SSTR2* mRNA expression levels were maximally enhanced after LMK-235 treatment. To the best of our knowledge, the HDACis used in our studies have not been tested in NCI-H69 cells before. In contrast, BON-1 cells are frequently used as a model for HDACi-induced SSTR2 upregulation. In our current study, we observed significant effects induced after PAN treatment, demonstrating stronger effects than that observed in NCI-H69 cells. Similarly to what was observed in NCI-H69 cells, the strongest effect was seen 24 h after start of treatment. Convincing *in vitro* results of HDACi treatment on SSTR2 expression in BON-1 cells have also been described in literature [14–16,20–23,33,34]. Based on our data and the data described in literature, it may be speculated that cells with low baseline SSTR2 expression levels are more susceptible to HDACi-induced SSTR2 upregulation. However, future studies focusing on this association are needed to confirm the link between baseline SSTR2 expression levels and the extent of SSTR2 upregulation.

Subsequently, the effects of all five HDACis were tested in NCI-H69 tumor-bearing animals. As *in vitro* effects were quickly induced, animals were treated on three consecutive days. Unfortunately, the tumoral uptake of radiolabeled DOTA-TATE was not significantly increased after HDACi treatment. However, SSTR2 expression levels were changed, *i.e.* increased *SSTR2* mRNA expression in MOC-, PAN- and CI-994-treated animals, and increased protein expression levels in CI-994-treated animals. In order to exclude possible model-dependent outcomes, we also tested the effect of PAN in BON-1 tumor-bearing animals. This HDACi was selected for several reasons. First, we observed convincing results *in vitro* in a previously published study following a seven day treatment [23]. Second, in the same study, it was demonstrated that increased *SSTR2* mRNA expression levels were maintained up to seven days after PAN withdrawal, potentially facilitating HDACi-induced SSTR2 upregulation *in vivo*. Third, PAN targets all classes of HDAC enzymes, thereby possibly having more potency to increase SSTR2 expression [35]. Despite the aforementioned, biodistribution results showed no increase in tumoral uptake of radiolabeled DOTA-TATE in this model. In line with what was observed in NCI-H69 tumor-bearing animals, tumoral *SSTR2* mRNA expression was significantly increased, but no increase in SSTR2 protein expression level was observed.

The obtained *in vivo* data acquired in our studies are thus somewhat puzzling. First, there is a discrepancy in CI-994-treated NCI-H69 animals demonstrating both an increase in SSTR2 mRNA and protein expression level, but no significant increase in radiolabeled DOTA-TATE uptake. It is likely that the increase in SSTR2 protein expression level, although significantly enhanced, is not sufficient to significantly increase [^{177}Lu]Lu-DOTA-TATE uptake as well, especially since NCI-H69 xenografts already have relatively high baseline SSTR2 expression levels. Therefore, it might be of value to optimize the HDACi dose and/or treatment duration to further increase tumoral SSTR2 expression levels which could potentially lead to a significantly enhanced uptake of radiolabeled DOTA-TATE. Secondly, we observed a discrepancy between *SSTR2* mRNA and protein expression levels after PAN treatment in both models as only mRNA expression levels were significantly elevated. It is difficult to exactly pinpoint the reason for this discrepancy based on the acquired data. We cannot exclude the possibility that PAN treatment alters biological processes *in vivo* causing the discrepancy between *SSTR2* mRNA and SSTR2 protein expression levels, *e.g.* inhibiting protein translation and/or inducing breakdown of proteins. However, this seems unlikely as it is contradictory to the results obtained in our *in vitro* studies. Furthermore, the method used to measure *SSTR2* mRNA and SSTR2 protein expression levels might contribute to this discrepancy. Whereas mRNA expression levels were measured by collecting several fresh frozen tissue slices, the quantification of SSTR2 protein expression level was based on three images within one FFPE tissue slice. Since NCI-H69 can have a heterogeneous phenotype [36], SSTR2 protein detection using IHC on one tissue slice can be less sensitive than *SSTR2* mRNA analysis. Thus, more in-depth investigations are needed to unravel the exact reason behind the observed discrepancy in *SSTR2* mRNA and SSTR2 protein expression levels.

In case further optimization of HDACi treatment would result in significantly higher tumoral uptake of radiolabeled SSA, certain factors should be kept in mind for survival and toxicity studies. For survival studies, it should be taken into account that HDACis, in addition to modulating gene transcription, have therapeutic value on their own as these drugs can induce apoptosis [37]. If an increased survival is observed after combination treatment (*i.e.* HDACi with radiolabeled DOTA-TATE), the mechanism-of-action should therefore be confirmed, *i.e.* an HDACi-mediated increase in radiolabeled SSA uptake instead of additive/synergistic effects of both monotherapies. Moreover, the safety of the combination treatment should be monitored in follow-up studies. Although histology assessment of the kidneys showed no HDACi-induced damage in our study, kidney function (*e.g.* creatinine levels and/or blood urea nitrogen) was not monitored. It might be of significance to also include the latter analysis in future studies.

Interestingly, differences in physiological uptake in NCI-H69 and BON-1 tumor-bearing animals were observed in our study which could possibly be caused by serotonin secreted by BON-1 tumor cells causing changes in vascular tone [38], resulting in a lower radioactivity uptake in the intestine, pancreas and stomach, and a higher radioactivity uptake in the kidneys of BON-1 tumor-bearing animals.

In addition to investigating the effects of HDACis on the uptake of radiolabeled SSA, we studied the association between *HDACs* and *SSTR2* expression levels. Overall, BON-1 xenografts demonstrated higher HDAC expression levels than NCI-H69 xenografts. More importantly, HDAC3, characterized by a significant inverse correlation with SSTR2 in our correlation analysis, was expressed higher in BON-1 than in NCI-H69 cells and xenografts. Remarkably, the higher HDAC expression levels in BON-1, in comparison to those measured in NCI-H69 cells, were associated with stronger effects observed after HDACi treatment in our *in vitro* studies. Of note, the correlation analysis was performed with mRNA expression levels, which does not necessarily match HDAC protein expression, nor HDAC enzyme activity. Additionally, it would have been of value to investigate the acetylation status in the SSTR2 promoter area *in vitro* and *in vivo* to further interpret our findings, as this could possibly explain the different results obtained *in vitro* and *in vivo*.

5. Conclusion

In conclusion, our *in vitro* results confirmed the currently available results on HDACi-induced SSTR2 upregulation. Unfortunately, despite increased SSTR2 mRNA and/or protein expression levels after HDACi treatment, no increase in tumoral uptake of radiolabeled DOTA-TATE was observed. Overall, our study highlights the complexity of applying epigenetic drugs for enhancing the tumoral radiolabeled SSA uptake, while it also indicates the potential of this combination treatment. Future studies are needed to gain more understanding on the mechanism-of-action of HDACis *in vivo*, including the relation between HDACi dose, SSTR2 expression and radiolabeled SSA uptake.

Ethics approval

This study was performed in line with the principles of the Declaration of Helsinki. Approval was granted by the Ethics Committee of the Erasmus Medical Center (SP2100386/21-04-2022 and SP2200197/29-11-2022).

Funding

This project is funded by an Erasmus MC grant (2017).

CRediT authorship contribution statement

Maria J. Klomp, Leo J. Hofland and Simone U. Dalm conceptualized of the study. Formal analysis was performed by Maria J. Klomp, Lilian van den Brink, Peter M. van Koetsveld, Corrina M.A. de Ridder and Debra C. Stuurman. Investigation was performed by Maria J. Klomp, Lilian van den Brink, Peter M. van Koetsveld, Corrina M.A. de Ridder and Debra C. Stuurman. All authors were responsible for the methodology. Leo J. Hofland and Simone U. Dalm were responsible for funding acquisition and resources. Clemens W.G.M. Löwik, Leo J. Hofland and Simone U. Dalm were responsible for supervision. The first draft of the manuscript was written by Maria J. Klomp and all authors commented on previous versions on the manuscript. All authors read and approved the final manuscript.

Declaration of competing interest

The authors declare no conflict of interest.

Data availability

The datasets generated during and/or analyzed during the current study are available from the corresponding author on reasonable request.

Acknowledgements

We are grateful for the Radiopharmaceutical Chemistry group (Radiology and Nuclear Medicine, Erasmus MC, The Netherlands) for radiolabeling of the tracers used in this study. We would also like to thank Marian C. Clahsen-van Groningen (Department of Pathology, Erasmus MC, The Netherlands) for evaluating the renal tubular damage score.

Appendix A. Supplemental Appendix

Supplementary data to this article can be found online at https://doi.org/10.1016/j.lfs.2023.122173.

References

[1] T. Günther, et al., International Union of Basic and Clinical Pharmacology. CV. Somatostatin receptors: structure, function, ligands, and new nomenclature, Pharmacol. Rev. 70 (4) (2018) 763–835.

[2] M. Pavel, et al., Gastroenteropancreatic neuroendocrine neoplasms: ESMO clinical practice guidelines for diagnosis, treatment and follow-up, Ann. Oncol. 31 (7) (2020) 844–860.

[3] J. Hofland, et al., Management of carcinoid syndrome: a systematic review and meta-analysis, Endocr. Relat. Cancer 26 (3) (2019) R145–R156.

[4] W.T. Zandee, et al., Peptide receptor radionuclide therapy with 177Lu-DOTATATE for symptomatic control of refractory carcinoid syndrome, J. Clin. Endocrinol. Metab. 106 (9) (2021) e3665–e3672.

[5] A. Rinke, et al., Placebo-controlled, double-blind, prospective, randomized study on the effect of octreotide LAR in the control of tumor growth in patients with metastatic neuroendocrine midgut tumors: a report from the PROMID Study Group, J. Clin. Oncol. 27 (28) (2009) 4656–4663.

[6] M.E. Caplin, et al., Lanreotide in metastatic enteropancreatic neuroendocrine tumors, N. Engl. J. Med. 371 (3) (2014) 224–233.

[7] J. Strosberg, et al., Phase 3 trial of (177)Lu-Dotatate for midgut neuroendocrine tumors, N. Engl. J. Med. 376 (2) (2017) 125–135.

[8] J.R. Strosberg, et al., (177)Lu-Dotatate plus long-acting octreotide versus high-dose long-acting octreotide in patients with midgut neuroendocrine tumours (NETTER-1): final overall survival and long-term safety results from an open-label, randomised, controlled, phase 3 trial, Lancet Oncol. 22 (12) (2021) 1752–1763.

[9] N.S. Minczeles, et al., Strategies towards improving clinical outcomes of peptide receptor radionuclide therapy, Curr. Oncol. Rep. 23 (4) (2021) 46.

[10] E. Klieser, et al., Comprehensive immunohistochemical analysis of histone deacetylases in pancreatic neuroendocrine tumors: HDAC5 as a predictor of poor clinical outcome, Hum. Pathol. 65 (2017) 41–52.

[11] A. Di Domenico, et al., Genetic and epigenetic drivers of neuroendocrine tumours (NET), Endocr. Relat. Cancer 24 (9) (2017) R315–R334.

[12] A. Mafficini, A. Scarpa, Genetics and epigenetics of gastroenteropancreatic neuroendocrine neoplasms, Endocr. Rev. 40 (2) (2019) 506–536.

[13] M.J. Klomp, et al., Epigenetic regulation of somatostatin and somatostatin receptors in neuroendocrine tumors and other types of cancer, Rev. Endocr. Metab. Disord. 22 (3) (2021) 495–510.

[14] L. Sun, et al., Valproic acid induces NET cell growth arrest and enhances tumor suppression of the receptor-targeted peptide-drug conjugate via activating somatostatin receptor type II, J. Drug Target. 24 (2) (2016) 169–177.

[15] M.J. Veenstra, et al., Epidrug-induced upregulation of functional somatostatin type 2 receptors in human pancreatic neuroendocrine tumor cells, Oncotarget 9 (19) (2018) 14791–14802.

[16] J. Kotzerke, et al., Epigenetic-like stimulation of receptor expression in SSTR2 transfected HEK293 cells as a new therapeutic strategy, Cancers (Basel) 14 (10) (2022).

[17] M.J. Klomp, et al., The effect of VPA treatment on radiolabeled DOTATATE uptake: differences observed in vitro and in vivo, Pharmaceutics 14 (1) (2022).

[18] J. Refardt, et al., Effect of epigenetic treatment on SST(2) expression in neuroendocrine tumour patients, Clin. Transl. Med. 12 (7) (2022), e957.

[19] J.H. Pollard, et al., Potential for increasing uptake of radiolabeled (68)Ga-DOTATOC and (123)I-MIBG in patients with midgut neuroendocrine tumors using a histone deacetylase inhibitor vorinostat, Cancer Biother. Radiopharm. 36 (8) (2021) 632–641.

[20] J. Wanek, et al., Pharmacological inhibition of class IIA HDACs by LMK-235 in pancreatic neuroendocrine tumor cells, Int. J. Mol. Sci. 19 (10) (2018).

[21] R.E. Guenter, et al., Pulmonary carcinoid surface receptor modulation using histone deacetylase inhibitors, Cancers (Basel) 11 (6) (2019).

[22] R. Guenter, et al., Overexpression of somatostatin receptor type 2 in neuroendocrine tumors for improved Ga68-DOTATATE imaging and treatment, Surgery 167 (1) (2020) 189–196.

[23] M.J. Klomp, et al., Comparing the effect of multiple histone deacetylase inhibitors on SSTR2 expression and [(111)In]In-DOTATATE uptake in NET cells, Cancers (Basel) 13 (19) (2021).

[24] E. Hessmann, et al., Epigenetic treatment of pancreatic cancer: is there a therapeutic perspective on the horizon? Gut 66 (1) (2017) 168–179.

[25] N. Tandon, V. Ramakrishnan, S.K. Kumar, Clinical use and applications of histone deacetylase inhibitors in multiple myeloma, Clin. Pharmacol. 8 (2016) 35–44.

[26] E. de Blois, et al., Application of single-vial ready-for-use formulation of 111In- or 177Lu-labelled somatostatin analogs, Appl. Radiat. Isot. 85 (2014) 28–33.

[27] A.M. El-Naggar, et al., Class I HDAC inhibitors enhance YB-1 acetylation and oxidative stress to block sarcoma metastasis, EMBO Rep. 20 (12) (2019), e48375.

[28] C. Bonfils, et al., Evaluation of the pharmacodynamic effects of MGCD0103 from preclinical models to human using a novel HDAC enzyme assay, Clin. Cancer Res. 14 (11) (2008) 3441–3449.

[29] S. Trazzi, et al., HDAC4: a key factor underlying brain developmental alterations in CDKL5 disorder, Hum. Mol. Genet. 25 (18) (2016) 3887–3907.

[30] A. Cooper, et al., Inhibition of histone deacetylation rescues phenotype in a mouse model of Birk-Barel intellectual disability syndrome, Nat. Commun. 11 (1) (2020) 480.

[31] E.M. Ocio, et al., In vitro and in vivo rationale for the triple combination of panobinostat (LBH589) and dexamethasone with either bortezomib or lenalidomide in multiple myeloma, Haematologica 95 (5) (2010) 794–803.

[32] C. Campana, et al., Digital quantification of somatostatin receptor subtype 2a immunostaining: a validation study, Eur. J. Endocrinol. 187 (3) (2022) 399–411.

[33] V.F. Taelman, et al., Upregulation of key molecules for targeted imaging and therapy, J. Nucl. Med. 57 (11) (2016) 1805–1810.

[34] X.F. Jin, et al., Combination of 5-fluorouracil with epigenetic modifiers induces radiosensitization, somatostatin receptor 2 expression, and radioligand binding in neuroendocrine tumor cells in vitro, J. Nucl. Med. 60 (9) (2019) 1240–1246.

[35] A. Singh, et al., Panobinostat as pan-deacetylase inhibitor for the treatment of pancreatic cancer: recent progress and future prospects, Oncol. Ther. 4 (1) (2016) 73–89.

[36] D. Feijtel, et al., Inter and intra-tumor somatostatin receptor 2 heterogeneity influences peptide receptor radionuclide therapy response, Theranostics 11 (2) (2021) 491–505.

[37] J. Zhang, Q. Zhong, Histone deacetylase inhibitors and cell death, Cell. Mol. Life Sci. 71 (20) (2014) 3885–3901.

[38] L.F. Mohammad-Zadeh, L. Moses, S.M. Gwaltney-Brant, Serotonin: a review, J. Vet. Pharmacol. Ther. 31 (3) (2008) 187–199.